IEEE Access
Multidisciplinary | Rapid Review | Open Access Journal

Received March 21, 2019, accepted April 16, 2019, date of publication April 25, 2019, date of current version May 6, 2019.

Digital Object Identifier 10.1109/ACCESS.2019.2913163

Remaining Useful Life Prediction of Lithium-Ion Batteries Using Neural Network and Bat-Based Particle Filter

YI WU, WEI LI, YOUREN WANG, AND KAI ZHANG
College of Automation Engineering, Nanjing University of Aeronautics and Astronautics, Nanjing 211106, China

Corresponding author: Yi Wu (janeyi105@126.com)

This work was supported in part by the National Natural Science Foundation of China under Grant 61371041, in part by the Funding for Outstanding Doctoral Dissertation in NUAA under Grant BCXJ14-04, in part by the Fundamental Research Funds for the Central Universities, and in part by the Funding of Jiangsu Innovation Program for Graduate Education under Grant KYLX 0251.

ABSTRACT Predicting the remaining useful life (RUL) is an effective way to indicate the health of lithium-ion batteries, which can help to improve the reliability and safety of battery-powered systems. To predict the RUL, the line of research focuses on using the empirical degradation model followed by the particle filter (PF) algorithm, which is used for online updating the model's parameters. However, this works well for specific batteries under specific discharge conditions. When the degradation trends cannot be presented by the chosen empirical model or the standard PF encounters impoverishment and degeneracy problem, the RUL prediction would be inaccurate. To improve the RUL prediction accuracy, we propose a novel approach by enhancing the existing method from two aspects. First, we introduce a neural network (NN) to model battery degradation trends under various operation conditions. As NN's generalization and nonlinear representing ability, it outperforms the typical empirical degradation model. Second, the NN model's parameters are recursively updated by the bat-based particle filter. The bat algorithm is used to move the particles to the high likelihood regions, which optimizes the particle distribution and thus reduces the degeneracy and impoverishment of PF. In this paper, quantitative evaluation is presented using two datasets with different batteries under different aging conditions. The results indicate that the proposed the approach can achieve higher RUL prediction accuracy than conventional empirical model and standard PF.

INDEX TERMS Lithium-ion batteries, neural network, capacity degradation, remaining useful life prediction, bat algorithm, particle filter.

I. INTRODUCTION

Lithium-ion batteries have been broadly used in transportation, aerospace, and defense military applications due to their low self-discharge rate, high operating voltage, long cycle life, and high energy density. The lithium-ion batteries are usually used to provide power for electrical systems, in other words, they store and then release electrical energy through internal electrochemical reactions. However, the battery suffers from side reactions during operation, which leads to materials aging and capacity fade of the battery, and thus cause performance degradation or even catastrophic events of electrical systems [1]. Therefore, predicting the remaining useful life (RUL) of lithium-ion batteries is critical and indispensable for the electrical systems. Accurate RUL prediction can effectively indicate lithium-ion batteries' health, which could help to provide maintenance plans to ensure the reliability and safety of the systems [2], [3].

Many approaches have been proposed to predict the RUL of lithium-ion batteries [4], which can be generally grouped into two families, the fully data-driven methods and the model-based methods. Note that hybrid approaches fused data-driven and model-based methods also gain lots of research interests recently [5]–[7]. Regarding the fully data-driven methods, the degradation features are extracted from the historical data such as voltage, current, and temperature. Then the machine learning algorithms are used to predict the degradation and estimate the RUL of the batteries. Typical data-driven approaches used for battery RUL prediction include auto regressive integrated moving average (ARIMA) model [8], Gaussian process regression (GPR) [9], long short-term memory recurrent neural

The associate editor coordinating the review of this manuscript and approving it for publication was Dong Wang.

network (LSTM RNN) [10], relevance vector machine (RVM) [11], [12]. The data-driven methods require completely historical data to fully train models, which is not always available in real-world systems. Besides, fully data-driven methods usually do not support prediction uncertainties. Thus, model-based RUL prediction methods, which modeling the degradation trends by a mathematical model and corresponding parameters, gain more attention recently. The degradation model can be further divided into physics of failure (PoF) model and empirical model. The PoF model is developed based on the knowledge of material properties, loading conditions and failure mechanisms of the batteries. However, it is hard to build an accurate PoF model because complicated electrochemical experiments and professional equipment are needed to identify the model parameters, which limits its generalization for on-board applications [13]. Instead, empirical models require less physical or electrochemical information of the batteries. They are usually established based on regression analysis of the battery degradation data.

Obviously, building a precise empirical model to capture the capacity or resistance fade behaviors is critical for accurate RUL prediction. Saha *et al.* [14] extracted the resistances from the electrochemical impedance spectroscopy (EIS) data and then performed RVM regression to build the exponential resistance growth model. He *et al.* [15] introduced a double exponential model to fit the battery degradation behavior and used this model to estimate the RUL. Xing *et al.* [16] presented a model that fuses He's model and a polynomial model to take account of both global and local degradation behaviors. Guha and Patra [17] proposed a model by combining an exponential capacity degradation model and a polynomial resistance growth model. Yang *et al.* [18] developed a logarithmic model for Li(NiMnCo)O_2 batteries, which have concave degradation trends. Wang *et al.* [19] developed a discharge-rate-dependent degradation model by extending an exponential model. All the above models are designed for the degradation behaviors under specific discharge conditions or for batteries with particular materials. In real-world applications, the batteries often work under non-nominal operating conditions. Thus, a general and flexible model, which can capture the capacity fade trend under varying operation conditions, is urgently desired for battery RUL prediction. Recently, the neural network (NN) has been successfully used in vast applications due to its powerful capability of generalization and representing the nonlinear behavior [20]. Regarding the RUL prediction, the NN has the potential to effectively deal with the nonlinear and dynamic degradation behavior of lithium-ion batteries.

To recursively update the parameters of the degradation model for online RUL prediction, filter techniques are usually adopted [21]. Among numbers of filter techniques, particle filter (PF) is widely used because it can deal with both non-Gaussian and nonlinear systems [15]–[18]. The insight of PF is to utilize a set of random particles with their importance weights to estimate the posterior probability density function (pdf) for the system states. However, the standard PF method suffers from particle degeneracy and impoverishment problems. Thus, some efforts have been made to tackle those problems by choosing different importance functions or resampling strategies [22], [23]. Miao *et al.* [24]–[26] introduced an unscented PF for battery RUL prediction. Ma *et al.* [27] developed a Gauss-Hermite PF to update the degradation model's parameters. Li *et al.* [28] proposed a mutated PF method to estimate the system states and implemented it for battery life prediction. Wang *et al.* [29] established a state-space model for battery degradation and employed the spherical cubature PF to estimate the battery life. As an alternative, intelligent PF is a promising approach to improve the robustness and effectiveness of PF. The essential of intelligent PF is utilizing metaheuristic algorithms to optimize the distribution of particles rather than simply delete the low weight particles [30] in resampling procedure, which effectively tackles the particle impoverishment problem. Several metaheuristic methods (such as particle swarm optimization [31], genetic algorithm, and firefly algorithm [32]) have been explored and proven to be able to enhance the standard PF in typical applications. Recently, a bat-inspired metaheuristic algorithm is proposed by Yang [33]. The bat algorithm is a random search mechanism with a stronger adaptive ability and better precision of convergence than conventional swarm-like particle swarm optimization algorithm. Therefore, it is promising to further improve the intelligent PF by integrating of the bat and the PF.

In this paper, an intelligent battery RUL prediction approach using the NN model and the bat-based PF (Bat-PF) is proposed. This approach improves the RUL prediction accuracy of the current PF based method from two aspects. Firstly, a general NN model is developed for capacity degradation modeling. The NN model is more flexible and powerful than existing empirical models, and thus improves the RUL prediction accuracy by precisely modeling various degradation trends. Secondly, the parameters (weights and biases) of the NN model are updated using Bat-PF, which enhances the PF method by the bat algorithm. The Bat-PF method moves the particles to high likelihood regions based on the new capacity data by simulating the movements of bats. This method optimizes the particle distribution more robust comparing to the standard PF, and thus further improves the prediction accuracy under complex conditions.

This paper is organized as follows. Section II introduces the developed NN capacity degradation model. Section III presents the theory of Bat-PF and the proposed RUL prediction method. Experiment results are discussed in section IV. Lastly, the conclusions are summarized in section V.

II. CAPACITY DEGRADATION MODEL

A. CAPACITY DATASETS

In our paper, two different datasets are considered to investigate the capacity degradation behavior and illustrate the

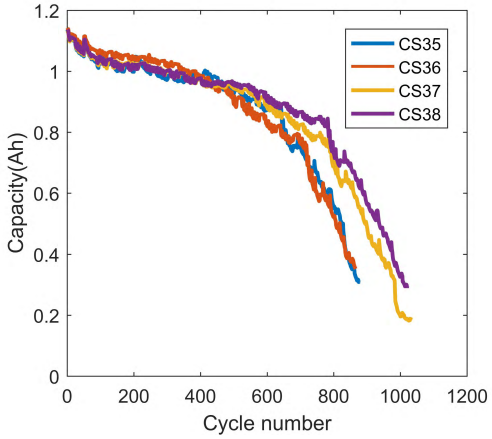

FIGURE 1. Capacity degradation curves of CALCE batteries.

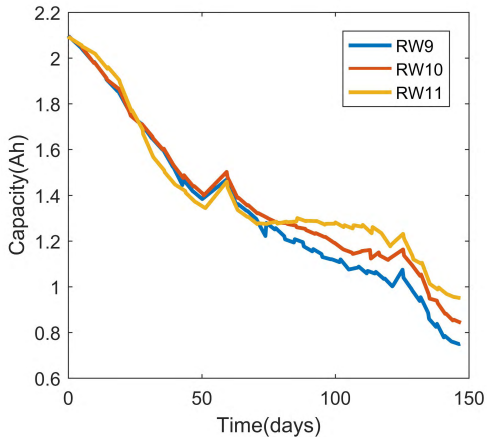

FIGURE 2. Capacity degradation curves of NASA batteries.

effectiveness of the developed degradation model and RUL prediction approach.

1) CALCE DATASET

The first dataset is from Center for Advanced Life Cycle Engineering (CALCE). Four $LiCoO_2$ pouch batteries (identified as CS35 to CS38) were cycled using an Arbin battery test system. The rated capacity is 1.1 Ah for those batteries. They were charged with a standard charging profile, and discharged at 1.1 A until the voltage fell to the cut-off voltage (2.7 V). The battery discharge capacity was obtained by Coulomb counting method. For those batteries, the failure threshold is recommended as 80% of the rated capacity [13]. The capacity degradation curve versus cycle is shown in Fig. 1. Since these batteries were cycled under constant load profiles, their capacities experience smooth fade trends, which form exponential curves in Fig. 1.

2) NASA DATASET

The second dataset is from NASA Ames Prognostics Center of Excellence [34]. To simulate the dynamic operation conditions in real applications, 18650 $LiCoO_2$ batteries (2.1 Ah) were cycled under a series of random currents rather than the constant discharge currents. Each loading period lasted for 5 minutes. A 2 A charging and discharging test was performed after every 1500 periods (about 5 days) to measure the battery capacity. For our study, we used the data from RW9 to RW11 batteries. Refer to [35], the failure thresholds for those batteries are considered as the capacities at the end of the test. The capacities are plotted against the test time (days) in Fig. 2. We can see that the capacity curve is highly dynamic and nonlinear.

B. NN DEGRADATION MODEL

Neural network gains huge success in recent years. With the powerful capability of generalization and representing, NN is widely used in various communities and proven to be able to solve complex problems effectively. In this paper, we utilize NN to model capacity degradation behavior. The basic unit

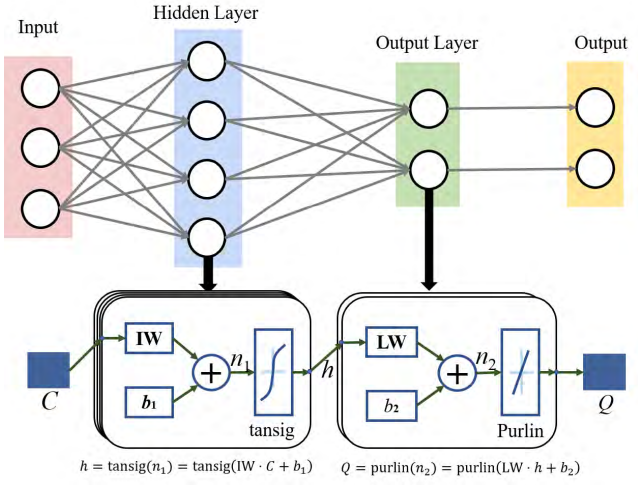

FIGURE 3. Structure diagram of a MLP model.

of a NN model is called neuron. Neurons are connected to form the layers of the neural network. Each neuron receives multiple inputs from other connected neurons in proportion to their weights. Then each neuron will generate a single output under activation function which may propagate to several other neurons. Among numerous NN variants or implementations, the multilayer perceptron (MLP), as a popular feed-forward NN, is characterized by simple structures [36]. Thus, MLP can be trained easily with rapid convergence while keeping conventional NN's capability of nonlinear approximation. In our case, to model the dynamic and nonlinear degradation trend of battery, MLP is the most attractive choice.

Fig. 3 shows the structure of a MLP model. The model consists of the input, hidden, and output layers. In our application, the network is used to model the capacity as the function of battery cycle. Thus, the input node is the cycle number or the cycle time (C), while the output node is the battery capacity (Q). The hyperbolic tangent sigmoid activation function (tansig) is adopted for the neurons in the hidden layer. The linear activation function (purelin) is employed for the

TABLE 1. Model parameters estimation results of EXP model and 2 neurons NN model for CALCE dataset.

Battery ID	EXP model				2 neurons NN model						
	φ_1	φ_2	φ_3	φ_4	IW_1	IW_2	LW_1	LW_2	b_{11}	b_{12}	b_2
CS35	-0.0017	0.0067	1.0669	-0.0002	-1.8650	2.2055	1.3182	-14.3543	1.7128	4.3969	13.6035
CS36	-0.0030	0.0061	1.1089	-0.0002	-2.7210	-0.6427	3.2209	1.8514	3.8544	0.8706	-4.0437
CS37	-0.0005	0.0074	1.0751	-0.0002	-1.1664	-2.5018	5.8692	3.0778	2.1107	-3.9433	-2.1669
CS38	-0.0002	0.0081	1.0740	-0.0002	-1.4146	-1.7543	7.7459	5.7190	2.5093	-3.4255	-1.4892

TABLE 2. Goodness-of-fit of different models for CALCE dataset.

Indices	RMSE			R^2		
Model	EXP	NN		EXP	NN	
		2 neurons	3 neurons		2 neurons	3 neurons
CS35	0.0197	0.0150	0.0142	0.9812	0.9892	0.9902
CS36	0.0181	0.0178	0.0138	0.9860	0.9864	0.9917
CS37	0.0149	0.0135	0.0127	0.9881	0.9902	0.9913
CS38	0.0169	0.0140	0.0132	0.9854	0.9900	0.9910

output node. Thereby, the output of each hidden neuron can be calculated as:

$$\begin{aligned} h &= \text{tansig}\left(\text{IW}\cdot C + b_1\right) \\ &= \frac{1-\exp\left[-2\left(\text{IW}\cdot C + b_1\right)\right]}{1+\exp\left[-2\left(\text{IW}\cdot C + b_1\right)\right]} \end{aligned} \tag{1}$$

where, IW and b_1 are the weight and bias associated with the input node (C).

Then, the output of whole network can be calculated as:

$$\begin{aligned} Q &= \text{purlin}\left(\text{LW}_1\cdot h_1 + \cdots + \text{LW}_M\cdot h_M + b_2\right) \\ &= \text{LW}_1\cdot\frac{1-\exp\left[-2\left(\text{IW}_1\cdot C + b_{11}\right)\right]}{1+\exp\left[-2\left(\text{IW}_1\cdot C + b_{11}\right)\right]} \\ &\quad + \cdots + \text{LW}_M\cdot\frac{1-\exp\left[-2\left(\text{IW}_M\cdot C + b_{1\,M}\right)\right]}{1+\exp\left[-2\left(\text{IW}_M\cdot C + b_{1M}\right)\right]} + b_2 \end{aligned} \tag{2}$$

where LW and b_2 are the weight and bias associated with the hidden neurons, M is the number of hidden neurons.

C. DEGRADATION ANALYSIS BASED ON DIFFERENT MODELS

In this section, the developed NN model, *i.e.*,the MLP model, is compared with the conventional empirical model in terms of capacity degradation modeling. Regarding the empirical model, as the double exponential model [15] is the most widely used one for RUL prediction, it (denoted as EXP model) is chosen for this comparison. Specifically, the EXP model can be expressed by two exponential functions:

$$Q = \varphi_1 * \exp\left(\varphi_2 * C\right) + \varphi_3 * \exp\left(\varphi_4 * C\right) \tag{3}$$

where, φ_1, φ_2, φ_3, and φ_4 are the model parameters.

The parameters of the EXP model are fitted using the nonlinear least square method in MATLAB curve fitting tool. For the evaluation of the NN model, two types of implementation are considered. Concretely, we evaluate the NN model with 2 hidden neurons (denoted as 2 neurons NN model) and 3 hidden neurons (denoted as 3 neurons NN model). The parameters of the NN models are obtained using the MATLAB nntrain tool. The R-square (R^2) and root mean square error (RMSE) are used to assess the goodness-of-fit of these models [16], which are defined in (4) and (5), respectively. Note that the higher is better in terms of R^2, while the lower is better in terms of RMSE.

$$R^2 = 1 - \frac{\sum_{i=1}^{n}\left(Q_{i,\text{real}} - Q_{i,\text{est}}\right)^2}{\sum_{i=1}^{n}\left(Q_{i,\text{real}} - Q_{\text{mean}}\right)^2} \tag{4}$$

$$\text{RMSE} = \sqrt{\frac{1}{n}\sum_{i=1}^{n}\left(Q_{i,\text{real}} - Q_{i,\text{est}}\right)^2} \tag{5}$$

where, $Q_{i,\text{real}}$ is the real capacity, $Q_{i,\text{est}}$ is the fitted capacity, and Q_{mean} is the mean of real capacity values.

1) DEGRADATION ANALYSIS FOR CALCE DATASET

Fig. 4 shows curve fitting results for CS35 and CS37 based on the EXP model and two NN models, respectively. All these models can successfully capture the capacity degradation trend for these two batteries. The parameters fitting results for all 4 batteries based on EXP model and 2 neurons NN model are shown in Table 1. While the goodness-of-fit results of different models are shown in Table 2. We can see that the RMSEs are less than 0.02 while the R^2 values are higher than 0.98, which indicates that all the models can fit the capacity degradation data well. The RMSEs of the 3 neurons NN model are the smallest while the R^2 values are the largest among three models for all batteries. This means the fit capability of the 3 neurons NN model is the best among three models. However, the performance of the 3 neurons NN model does not improve significantly and the performance of the 2 neurons NN model and EXP model are acceptable in this case, because the capacity curves for those batteries are relatively smooth and follow the exponential degradation trends.

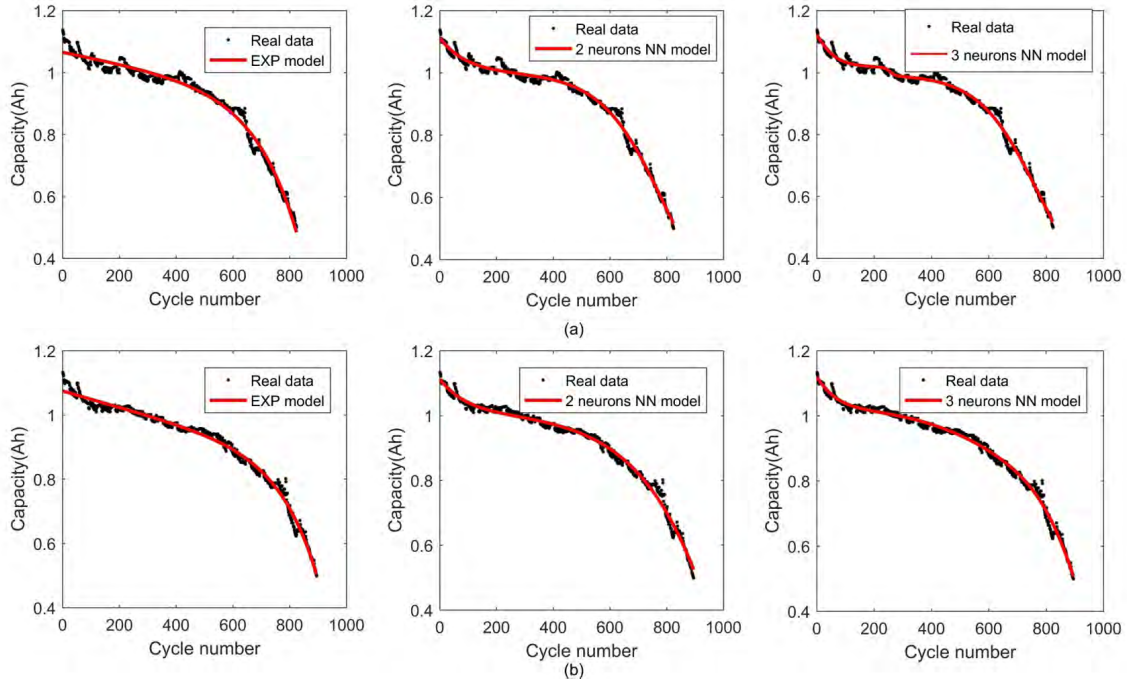

FIGURE 4. Curve fitting results for CALCE dataset: (a) CS35, and (b) CS37.

TABLE 3. Goodness-of-fit of different models for NASA dataset.

Indices	RMSE			R^2		
Model	EXP	NN		EXP	NN	
		2 neurons	3 neurons		2 neurons	3 neurons
RW9	0.0488	0.0311	0.0279	0.9823	0.9924	0.9939
RW10	0.0497	0.0307	0.0313	0.9775	0.9911	0.9906
RW11	0.0717	0.0280	0.0273	0.9425	0.9907	0.9912

2) DEGRADATION ANALYSIS FOR NASA DATASET

Fig. 5 shows curve fitting results for RW9 to RW11 based on the EXP model and NN models. The EXP model can only fit the first two-thirds of the data for RW9 and RW10. Moreover, the EXP model cannot track the whole degradation for RW11. Note that the poor-fitting of EXP model is due to the random fluctuation in capacity. However, we can see that the 2 neurons and 3 neurons NN models can both fit the whole life data.

Table 3 shows the goodness-of-fit statistics of different models. It can be found that the NN models have larger R^2 values and smaller RMSEs than the EXP model, which means the NN models show better global regression performance than the EXP model. For RW10, the 2 neurons model outperforms the 3 neurons model.

According to the degradation modeling analysis on those two datasets, the EXP model can only fit the degradation data whose trend is satisfied with the model assumption. However, the fitting results indicate the proposed NN model is suitable to describe the nonlinear degradation behavior of the battery cycled under different conditions. The performances of the 2 neurons and 3 neurons model show no much difference. Theoretically, the more hidden neurons used, the higher capability of the model can be achieved in terms of tracking the complex degradation trend. However, a large number of hidden neurons may cause overfitting problems. Furthermore, more hidden neurons mean more parameters to be optimized, *i.e.*, more computing complexity, during the initial training and the PF updating. Thus, we choose 2 hidden neurons model in our RUL prediction method.

III. RUL PREDICTION BASED ON BAT-PF

In the last section, we propose and evaluate the accuracy of the degradation model. However, to predict the RUL in an online manner, the model parameters should be updated step-by-step (each cycle). A typical solution for such online parameters adjustment is PF and related methods. Here, we first introduce the PF theory in section III-A. Next, we propose an enhanced PF method by metaheuristic bat algorithm (Bat-PF) in section III-B. Last, we describe our Bat-PF based RUL prediction approach in detail in section III-C.

A. STANDARD PARTICLE FILTER

PF is a state estimation method based on Monte Carlo and recursive Bayesian algorithm. In general, the state-space model for a dynamic system can be expressed by:

$$x_k = \mathcal{F}(x_{k-1}) + w_k \leftrightarrow p(x_k|x_{k-1}) \tag{6}$$

$$z_k = \mathcal{H}(x_k) + v_k \leftrightarrow p(z_k|x_k) \tag{7}$$

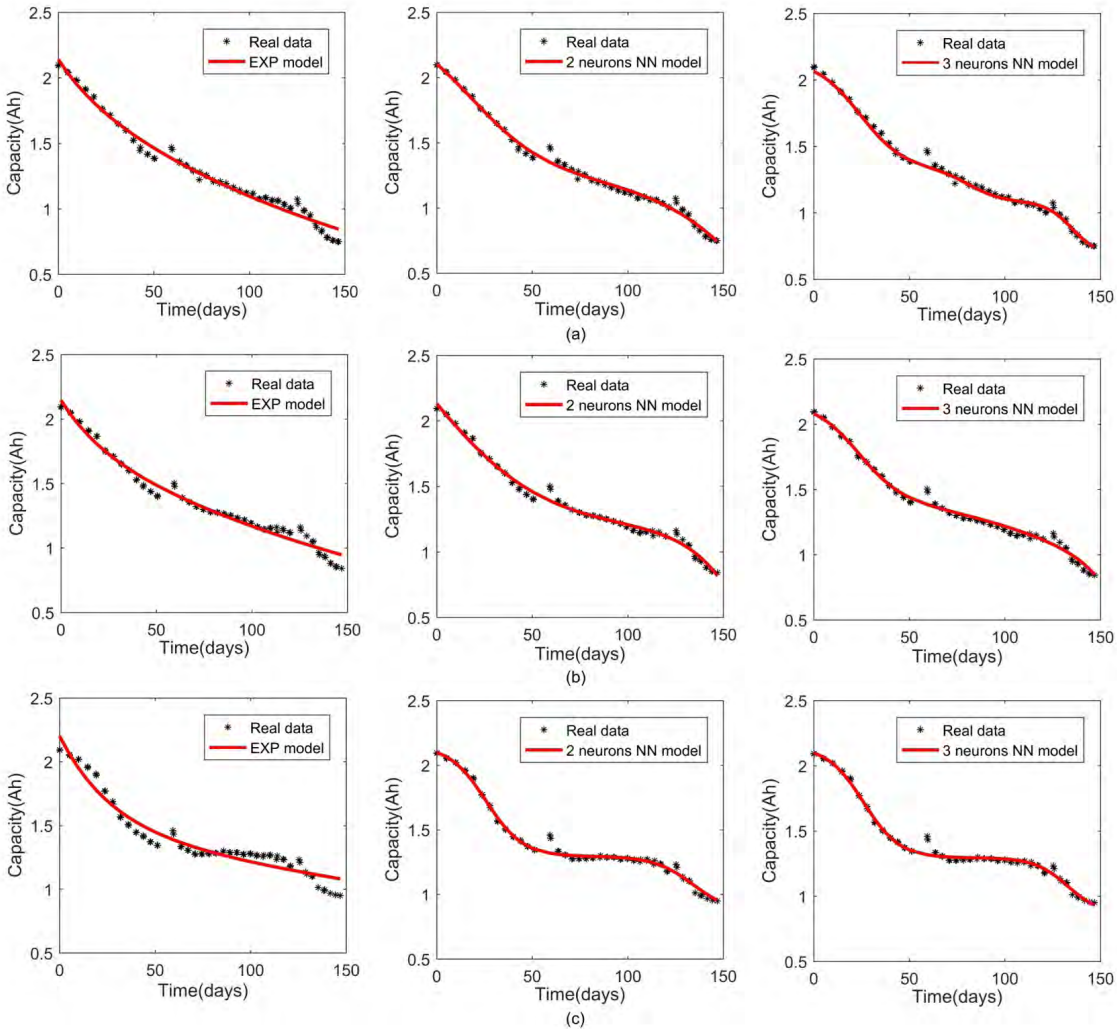

FIGURE 5. Curve fitting results for NASA dataset: (a) RW9, (b) RW10, and (c) RW11.

where, x_κ is the system state, w_κ denotes the process noise, z_κ is the observed vector, v_κ represents the measurement noise, κ is the sampling point, $\mathcal{F}$ is the state transition function, and $\mathcal{H}$ is the measurement function.

In PF algorithm, random particles are generated from the importance function $q\left(x_\kappa|z_{1:\kappa}\right)$ using Monte Carlo method. Denote x_κ^i is the i_{th} particle, and ω_κ^i is its associated weight. Then the posterior pdf $p\left(x_\kappa|z_{1:\kappa}\right)$ can be estimated by those weighted particles [37]:

$$p\left(x_\kappa|z_{1:\kappa}\right) \approx \sum_{i=1}^{N} \omega_\kappa^i \delta\left(x_\kappa - x_\kappa^i\right) \tag{8}$$

where N is the number of particles, $\delta(\cdot)$ is the Dirac delta function.

The importance function $q\left(x_\kappa|z_{1:\kappa}\right)$ highly relies on the newest measurement z_κ and the previous state $x_{\kappa-1}$. In battery RUL prediction applications, the prior pdf $p(x_\kappa^i|x_{\kappa-1}^i)$ is usually selected as the importance function to simplify the calculation of weights:

$$q\left(x_\kappa^i|x_{\kappa-1}^i, z_\kappa\right) = p\left(x_\kappa^i|x_{\kappa-1}^i\right) \tag{9}$$

Thus, the weight of each particle can be calculated as follows:

$$\omega_\kappa^i = \omega_{\kappa-1}^i \frac{p\left(z_\kappa|x_\kappa^i\right) p\left(x_\kappa^i|x_{\kappa-1}^i\right)}{q\left(x_\kappa^i|x_{\kappa-1}^i, z_\kappa\right)} = \omega_{\kappa-1}^i p\left(z_\kappa|x_\kappa^i\right) \tag{10}$$

where, $p(z_\kappa|x_\kappa^i)$ is the condition likelihood of x_κ^i.

B. BAT-PF

A common problem of the standard PF is the particle degeneracy, that is most of the particles having negligible weights after several iterations. A typical solution to this problem is resampling. The insight of resampling is to remove low-weight particles and fill up with duplicated high-weight particles. However, this will cause particle impoverishment and influence the accuracy of state estimation. Another problem of the PF is that it uses the prior distribution as the

importance function without considering the newest measurement. If the newest measurement has meaningful influences on the importance function, the estimated state will become unreliable and inaccurate.

To solve those problems and improve the accuracy of PF based RUL prediction, we propose a new method by integrating the bat algorithm into the PF. Bat is a population-based random search algorithm that imitates the behavior of micro-bats. In brief, the behavior of micro-bats can be mathematically modeled by flying randomly with velocity v at position x with a varying frequency f hunting for prey [38]. Micro-bats can automatically adjust their loudness A and the emission rate of pulse r during the hunting.

The core idea of the bat based PF is that after random drawn the particles from the prior distribution, each particle will be optimized by bat towards the high likelihood region in the state space. Then, those optimized particles are used for state estimation without resampling process. Besides, the key of the approach is the design of the objective function, which is used to evaluate each particle's position [38]. By introducing the newest observed value (z_k) into the particle optimization process, we define the objective function for bat using the exponential function as follows:

$$\text{Minimize} : I(x_\kappa) = \exp\left[-\frac{1}{2R}\left(z_\kappa - \bar{z}_\kappa\right)\right] \tag{11}$$

where, $\bar{z}_\kappa$ is the predicted value of the newest observed value z_κ, R is the standard deviation of measurement noise v in (7).

The main steps of Bat-PF are described as follows:

1) INITIALIZATION

Generate N particles $\{x_\kappa^i\}_{i=1}^N$ from the prior distribution using (6) as the initial particle swarm in bat. Each particle is randomly assigned a frequency f_i from $[f_{\min}, f_{\max}]$, a loudness $A_i(0)$ and an emission rate $r_i(0)$. Note that $f_{\max}$ and $f_{\min}$ are the maximum and minimum frequency, respectively.

2) PARTICLE OPTIMIZATION

During the n_{th} optimization iteration, the position and velocity of the i_{th} bat are updated as follows:

$$f_i = f_{\min} + (f_{\max} - f_{\min})\,\beta \tag{12}$$

$$v_i(n) = v_i(n-1) + (x_i(n-1) - x_{\text{best}})\,f_i \tag{13}$$

$$x_\kappa^i(n) = x_\kappa^i(n-1) + v_i(n) \tag{14}$$

where β is randomly chosen from $[0, 1]$, x_{best} is the best position.

Evaluate the solutions for each particle using the objective function (11). Generate a random number ($rand_1$) from a uniform distribution $[0, 1]$. If $rand_1 < r_i(n-1)$, the new solution of the i_{th} bat will be generated using (14). Otherwise, the new solution should be generated around the best solution by adding a random disturbance:

$$x_{\text{new}} = x_{\text{old}} + \varepsilon A' \tag{15}$$

where ε is a random number in $[0, 1]$, A^t is the average loudness for all bats.

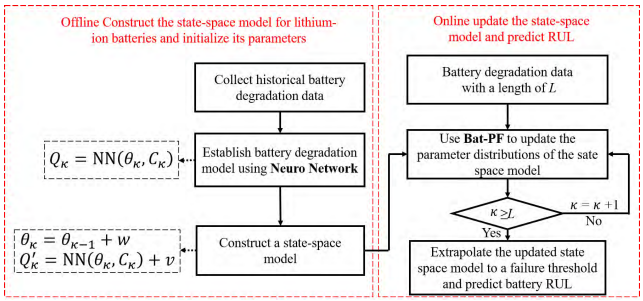

FIGURE 6. Flowchart of the proposed RUL prediction method for lithium-ion batteries.

Generate another random number ($rand_2$) from a uniform distribution $[0, 1]$. If $rand_2 < A_i(n-1)$ and the new solution is better than the old one, accept the new solution and adjust the corresponding loudness and the emission rate.

$$A_i(n) = \alpha A_i(n-1) \qquad (0 < \alpha < 1) \tag{16}$$

$$r_i(n) = r_i(0)[1 - \exp(-\gamma n)] \qquad (\gamma > 0) \tag{17}$$

where α and γ are constants, $r_i(0)$ is the initial emission rate.

3) OUTPUT THE STATES

If the maximum search iteration is reached or the search accuracy is satisfied, update the weights using (10), normalize the weights and output the states.

C. RUL PREDICTION METHOD

With the proposed NN degradation model and the novel Bat-PF algorithm, the RUL of lithium-ion batteries can be predicted in an online manner. Fig. 6 shows the flowchart of our RUL prediction method. Based on the capacity degradation data of the historical batteries, a state-space model is constructed based on the NN degradation model. Then, the Bat-PF is used to adjust the states (*i.e.*, the parameters of the degradation model). After that, the updated degradation model is extrapolated to the failure threshold to estimate the RUL. The detailed steps are described below.

1) CONSTRUCT THE STATE-SPACE MODEL

The weights and biases of the 2 neurons NN model are selected as the system states,*i.e.*, $[\text{IW}_1, \text{IW}_2, b_{11}, b_{12}, \text{LW}_1, \text{LW}_2, b_2]$. These 7 states are assumed to follow the random walk mode. Note the battery capacity is the measured vector. Thus, the state-space model can be constructed as follows:

$$\theta_\kappa = \begin{bmatrix} \text{IW}_{1,\kappa} \\ \text{IW}_{2,\kappa} \\ b_{11,\kappa} \\ b_{12,\kappa} \\ \text{LW}_{1,\kappa} \\ \text{LW}_{2,\kappa} \\ b_{2,\kappa} \end{bmatrix} = \begin{bmatrix} \text{IW}_{1,\kappa-1} \\ \text{IW}_{2,\kappa-1} \\ b_{11,\kappa-1} \\ b_{12,\kappa-1} \\ \text{LW}_{1,\kappa-1} \\ \text{LW}_{2,\kappa-1} \\ b_{2,\kappa-1} \end{bmatrix} + \begin{bmatrix} w_1 \\ w_2 \\ w_3 \\ w_3 \\ w_5 \\ w_6 \\ w_7 \end{bmatrix}, \begin{matrix} w_1 \sim (0, \sigma_1^2) \\ w_2 \sim (0, \sigma_2^2) \\ w_3 \sim (0, \sigma_3^2) \\ w_4 \sim (0, \sigma_4^2) \\ w_5 \sim (0, \sigma_5^2) \\ w_6 \sim (0, \sigma_6^2) \\ w_7 \sim (0, \sigma_7^2) \end{matrix} \tag{18}$$

$$Q'_\kappa = \mathrm{NN}(\theta_\kappa, \kappa) + v, \quad v \sim \left(0, \sigma_v^2\right) \tag{19}$$

where, NN(·) is the NN degradation model, all the noise (w_1 to w_7, v) are assumed to obey Gaussian distribution.

2) UPDATE THE STATES BASED ON BAT-PF

In this paper, the prior information for the states (*i.e.*, NN model parameters) in the PF algorithm is obtained from the database of the historical batteries which have the same specification with the test battery. The NN model parameters are initialized by training the degradation model using the data from historical samples. Then, the parameters can be updated using the constructed state-space model and Bat-PF as described in section III-B based on the available capacity data of the test battery. After obtained the posterior distribution of the model parameters $\{\theta_\kappa^i, \omega_\kappa^i\}_{i=1}^N$, the capacity at κ can be estimated as:

$$Q_\kappa = \sum_{i=1}^{N} \omega_\kappa^i Q_\kappa^i = \sum_{i=1}^{N} \omega_\kappa^i \mathrm{NN}\left(\theta_\kappa^i, C_\kappa\right) \tag{20}$$

3) RUL PREDICTION

By extrapolating the NN degradation model, the capacity at $\kappa + l$ can be predicted as:

$$Q_{\kappa+l} = \sum_{i=1}^{N} \omega_\kappa^i Q_{\kappa+l}^i = \sum_{i=1}^{N} \omega_\kappa^i \mathrm{NN}\left(\theta_\kappa^i, C_{\kappa+l}\right) \tag{21}$$

Then, the RUL of the i_{th} particle at κ (RUL_κ^i) can be estimated according to:

$$\mathrm{NN}\left(\theta_\kappa^i, C_\kappa + \mathrm{RUL}_\kappa^i\right) = threshold \tag{22}$$

The posterior pdf of the RUL at κ is approximated by:

$$p\left(\mathrm{RUL}_\kappa | Q_{1:\kappa}\right) \approx \sum_{i=1}^{N} \omega_\kappa^i \delta\left(\mathrm{RUL}_\kappa - \mathrm{RUL}_\kappa^i\right) \tag{23}$$

The expectation of RUL can be estimated by:

$$\mathrm{RUL}_\kappa = \sum_{i=1}^{N} \omega_\kappa^i \mathrm{RUL}_\kappa^i \tag{24}$$

IV. RESULTS AND DISCUSSION

The datasets from CALCE and NASA are used to evaluate the accuracy and robustness of the developed RUL prediction method. The following three methods are used for comparative analysis: the combination of EXP model and standard PF (EXP+PF), the combination of NN model and standard PF (NN+PF), and the combination of NN model and Bat-PF (NN+Bat-PF). The absolute error (AE) as shown in (25) is utilized to assess the accuracy of RUL prediction. The pdf width (PW) as shown in (26) is used to quantify the confidence level of RUL predictions [39]. A smaller pdf width indicates a more reliable RUL prediction.

$$\mathrm{AE} = \left|\mathrm{RUL}_{\kappa,\,\mathrm{real}} - \mathrm{RUL}_{\kappa,\,\mathrm{pred}}\right| \tag{25}$$

TABLE 4. Comparative analysis of different prediction methods for CS37.

Prediction cycles	Method	Real RUL	Predicted RUL	AE	90% CI	Pdf width
300	EXP+PF	302	426.00	124.00	[618.90,984.30]	365.00
	NN+PF		251.00	51.00	[521.00,678.00]	157.00
	NN+BAT-PF		256.00	46.00	[537.50,577.00]	39.50
400	EXP+PF	202	286.00	84.00	[600.00,827.00]	227.00
	NN+PF		163.00	39.00	[543.00,590.50]	47.50
	NN+BAT-PF		173.00	29.00	[548.00,599.50]	51.50
500	EXP+PF	102	161.00	59.00	[618.45,743.00]	124.55
	NN+PF		95.00	7.00	[576.50,617.50]	41.00
	NN+BAT-PF		100.00	2.00	[583.50,618.50]	35.00

where $\mathrm{RUL}_{\kappa,\,\mathrm{real}}$ is the real RUL at prediction point κ, and the $\mathrm{RUL}_{\kappa,\,\mathrm{pred}}$ is the predicted RUL.

$$\mathrm{PW} = U_{ci} - L_{ci} \tag{26}$$

where U_{ci} and L_{ci} are the upper and lower bounds of 95% confidence interval (CI) of RUL prediction result, respectively.

A. RESULTS FOR CALCE DATASET

Batteries CS35, CS36, and CS38 are arbitrarily selected as the historical batteries to provide prior information for model initialization, while CS37 is used to test the RUL prediction performance. Model initialization includes initializing the parameters and the corresponding variance. For the EXP model, the average values of the curve fitting results for the historical batteries' capacity data are used as the initial model parameters. The initial weights and biases of the NN model are obtained by training the network based on all the historical data. The noise variances are driven by the order of magnitudes of the variables in the state-space model, but they may vary from case to case. After the initialization, the parameters can be updated based on the newly measured capacity and the RUL can be predicted. Here, the particles number N is set as 100.

The RUL of CS37 is predicted from different cycles (*i.e.*, cycle 300, cycle 400, cycle 500, respectively). Fig. 7 to Fig. 9 show the RUL prediction for CS37 using EXP+PF, NN+PF and NN+Bat-PF, respectively. The black line is the real capacity. The red dotted line denotes the estimated capacity, and the red solid line shows the predicted curve. The black dotted line is the failure threshold. The yellow area denotes the predicted RUL pdf. As we can see from those figures, with more degradation capacity data obtained, the prediction curves gradually approach the true curve for all three methods, which indicates that the model parameters are correctly updated.

We can observe that the prediction curves obtained by NN models (Fig. 8 and Fig. 9) are closer to the real capacity degradation curve than using the EXP model (Fig. 7) at the same prediction point. Also, the RUL pdfs obtained using

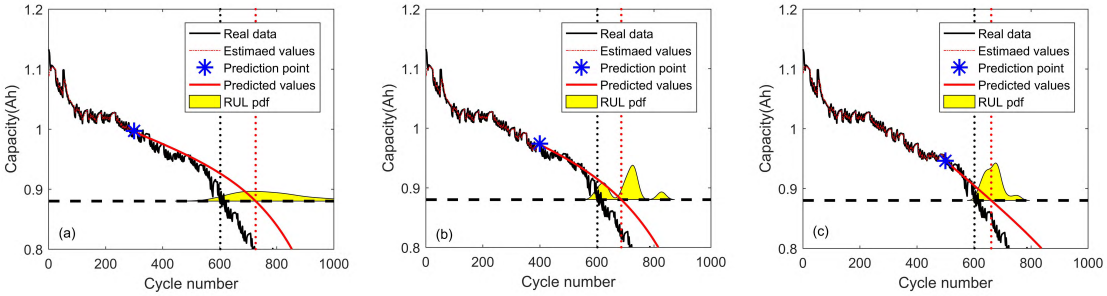

FIGURE 7. Prediction based on EXP+PF at different cycles for CS37: (a) T=300, (b) T=400, and (c) T=500.

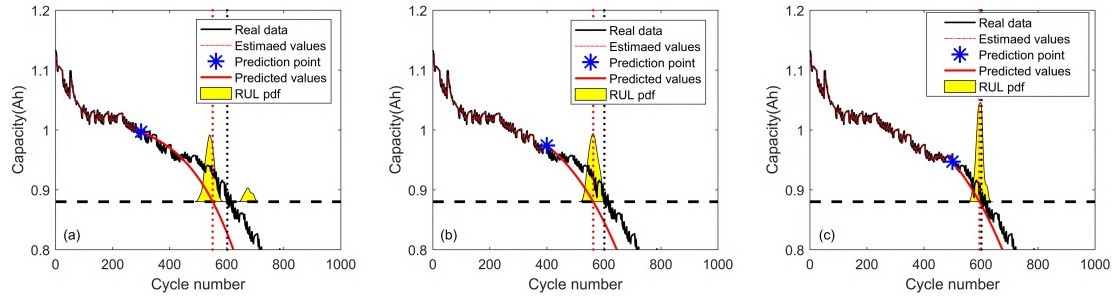

FIGURE 8. Prediction based on NN+PF at different cycles for CS37: (a) T=300, (b) T=400, and (c) T=500.

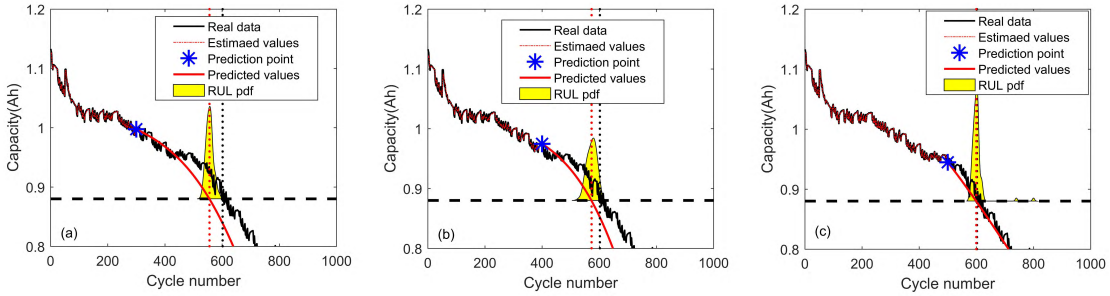

FIGURE 9. Prediction based on NN+Bat-PF at different cycles for CS37: (a) T=300, (b) T=400, and (c) T=500.

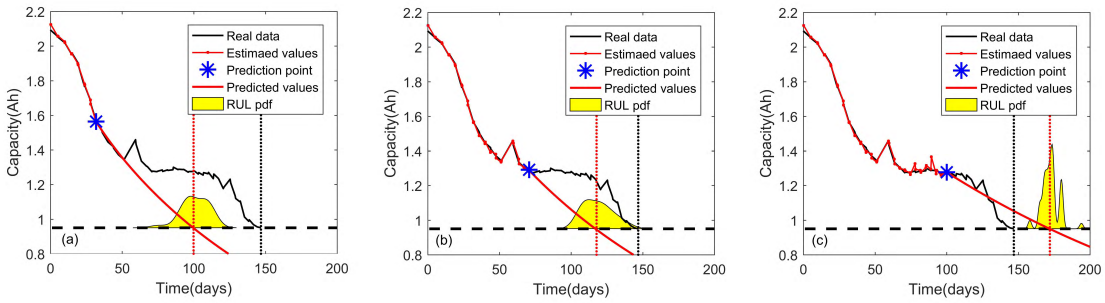

FIGURE 10. Prediction based on EXP+PF at different times for RW11: (a) T=30, (b) T=70, and (c) T=100.

NN models are narrower and taller than that obtained by the EXP model. Detailed quantitative results are listed in Table 4. Both the prediction errors and the RUL pdf widths in Table 4 suggest a relatively higher accuracy of the proposed NN degradation model than the EXP model. The reason for this result is that the NN model can better track the battery fade trend and consequently offer a more accurate state-space model for the RUL prediction framework.

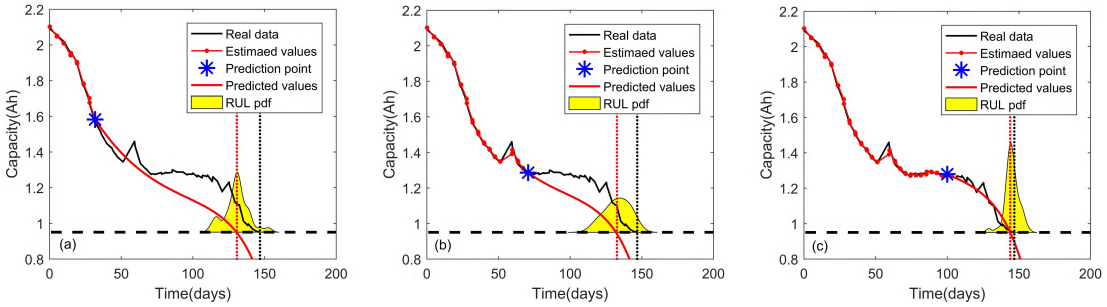

FIGURE 11. Prediction based on NN+PF at different times for RW11: (a) T=30, (b) T=70, and (c) T=100.

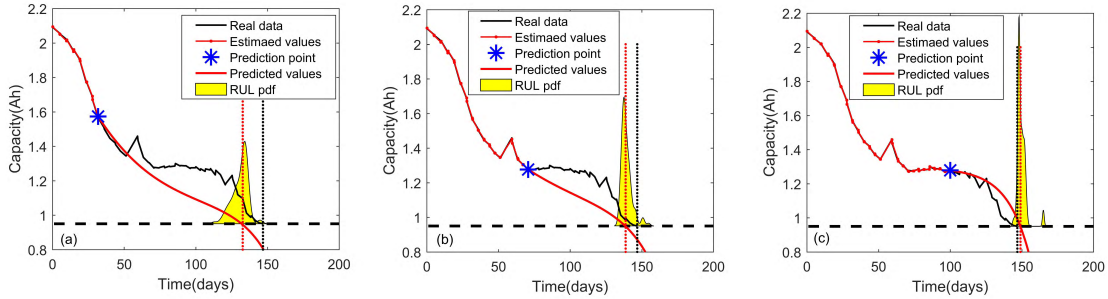

FIGURE 12. Prediction based on NN+Bat-PF at different times for RW11: (a) T=30, (b) T=70, and (c) T=100.

TABLE 5. Comparative analysis of different prediction methods for RW11.

Prediction days	Method	Real RUL	Predicted RUL	AE	90% CI	Pdf width
31.78	EXP+PF	115.05	68.00	47.05	[85.00,115.00]	30.00
	NN+PF		99.00	16.05	[116.78,146.28]	29.50
	NN+BAT-PF		101.00	14.05	[120.78,137.28]	16.50
70.76	EXP+PF	76.07	47.00	29.07	[109.00,139.00]	30.00
	NN+PF		62.00	14.07	[117.76,145.76]	28.00
	NN+BAT-PF		68.00	8.07	[135.26,145.35]	10.09
100.02	EXP+PF	46.81	72.00	25.19	[165.00,180.00]	15.00
	NN+PF		44.00	2.81	[139.02,153.02]	14.00
	NN+BAT-PF		49.00	2.19	[147.02,153.05]	6.03

It can also be found that NN+Bat-PF has lower AE, and narrower pdf width as compared to the NN+PF method in all prediction cycles, except for the pdf width at cycle 400. Using the numerical prediction results at cycle 500 for illustration, the RUL prediction error of the NN+Bat-PF is decreased by 5 cycles than that of NN+PF. The RUL pdf width of NN+PF is 41 cycles, which is larger than that of NN+Bat-PF (35 cycles). This result indicates that Bat-PF has not only better prediction accuracy but also less prediction uncertainty than PF.

B. RESULTS FOR NASA DATASET

For the NASA dataset, RW9 and RW10 are trained to obtain the initial model parameters, and RW11 is selected as the test battery. The RUL of RW11 is also predicted from different days. Fig. 10 to Fig. 12 are the RUL prediction results for RW11 using different methods. As we can see from Fig. 11 and Fig. 12, the prediction results based on NN methods show the desirable properties, that is the prediction curves can converge to the real capacity curves and the RUL pdfs become narrow as the time of prediction advances. Especially, in Fig. 11(c) and Fig. 12(c), the NN method tracks the aging variation well when collected the data after sudden changes (100 days). This is because by adjusting the model parameters using more capacity data, the NN model can effectively track the degradation trend and accordingly, achieve good prediction results. However, the capacity prediction curves obtained by the EXP model shown in Fig. 10 are obviously different from the real ones for all prediction times. The reason is that the degradation characteristic for this battery is relatively complex with strong dynamic. Thus, it is difficult to be tracked and predicted using the simple EXP model. The aforementioned analysis is in line with the prediction results in Table 5.

The detailed comparison results between Bat-PF and PF are also shown in Table 5. Similar to the prediction results for CALCE dataset, the Bat-PF method can obtain smaller prediction errors and narrower pdf widths than the standard PF at different prediction times, indicating the Bat-PF improves the prediction performance. For example, the RUL prediction error of NN+PF is 2.81 days and that of NN+Bat-PF is 2.19 days at 100.02 days, and the pdf width of NN+Bat-PF is 7.97 days smaller than that of NN+PF.

V. CONCLUSION

The accuracy of RUL prediction of lithium-ion batteries depends on both the degradation model and the online model updating method. In this paper, we propose a novel intelligent RUL prediction approach using the NN degradation model and Bat-PF. Comparing with the conventional empirical model, the proposed NN model has no requirement on the degradation pattern and can be adapted to various dynamic trends, which achieves better performance. On the other hand, by integrating the bat algorithm with the standard PF, we introduce a promising Bat-PF method to online update the degradation model parameters and estimate the RUL. Benefiting from the unique mechanism of the bat algorithm, which utilizes the newly capacity data to improve the PF particle distribution by moving the particles to high likelihood locations, our proposed Bat-PF method avoids the resampling process and thus prevents the particle degeneracy and impoverishment problem in standard PF method. Furthermore, we quantitatively evaluate the proposed NN model and Bat-PF method using two representative datasets, which are collected under different cycling conditions. The experimental results indicate that our method can better model the capacity degradation trend and obtain a higher RUL prediction accuracy (small prediction error and narrower pdf width) compared with conventional methods.

In future work, we are interested in extending our prediction method to more practical based applications. On the other hand, by exploring the relationship between the degradation model and the operation conditions, such as the working temperature and current, we also plan to build a general degradation model.

REFERENCES

[1] C. Hendricks, N. Williard, S. Mathew, and M. Pecht, "A failure modes, mechanisms, and effects analysis (FMMEA) of lithium-ion batteries," *J. Power Sources*, vol. 297, pp. 113–120, Nov. 2015.

[2] K. Javed, R. Gouriveau, and N. Zerhouni, "State of the art and taxonomy of prognostics approaches, trends of prognostics applications and open issues towards maturity at different technology readiness levels," *Mech. Syst. Signal Process.*, vol. 94, pp. 214–236, Sep. 2017.

[3] Y. Zhang, R. Xiong, H. He, and M. Pecht, "Validation and verification of a hybrid method for remaining useful life prediction of lithium-ion batteries," *J. Cleaner Prod.*, vol. 212, pp. 240–249, Mar. 2019.

[4] M. H. Lipu *et al.*, "A review of state of health and remaining useful life estimation methods for lithium-ion battery in electric vehicles: Challenges and recommendations," *J. Cleaner Prod.*, vol. 205, pp. 115–133, Dec. 2018.

[5] Y. Chang, H. Fang, and Y. Zhang, "A new hybrid method for the prediction of the remaining useful life of a lithium-ion battery," *Appl. Energy*, vol. 206, pp. 1564–1578, Nov. 2017.

[6] C. Hu, H. Ye, G. Jain, and C. Schmidt, "Remaining useful life assessment of lithium-ion batteries in implantable medical devices," *J. Power Sources*, vol. 375, pp. 118–130, Jan. 2018.

[7] L. Liao and F. Köttig, "A hybrid framework combining data-driven and model-based methods for system remaining useful life prediction," *Appl. Soft Comput.*, vol. 44, pp. 191–199, Jul. 2016.

[8] Y. Zhou and M. Huang, "Lithium-ion batteries remaining useful life prediction based on a mixture of empirical mode decomposition and ARIMA model," *Microelectron. Rel.*, vol. 65, pp. 265–273, Oct. 2016.

[9] D. Liu, J. Pang, J. Zhou, Y. Peng, and M. Pecht, "Prognostics for state of health estimation of lithium-ion batteries based on combination Gaussian process functional regression," *Microelectron. Rel.*, vol. 53, no. 6, pp. 832–839, 2013.

[10] Y. Zhang, R. Xiong, H. He, and M. G. Pecht, "Long short-term memory recurrent neural network for remaining useful life prediction of lithium-ion batteries," *IEEE Trans. Veh. Technol.*, vol. 67, no. 7, pp. 5695–5705, Jul. 2018.

[11] C. Zhang, Y. He, L. Yuan, and S. Xiang, "Capacity prognostics of lithium-ion batteries using EMD denoising and multiple kernel RVM," *IEEE Access*, vol. 5, pp. 12061–12070, 2017.

[12] D. Liu, J. Zhou, D. Pan, Y. Peng, and X. Peng, "Lithium-ion battery remaining useful life estimation with an optimized relevance vector machine algorithm with incremental learning," *Measurement*, vol. 63, pp. 143–151, Mar. 2015.

[13] Z. Liu, G. Sun, S. Bu, J. Han, X. Tang, and M. Pecht, "Particle learning framework for estimating the remaining useful life of lithium-ion batteries," *IEEE Trans. Instrum. Meas.*, vol. 66, no. 2, pp. 280–293, Feb. 2017.

[14] B. Saha, K. Goebel, S. Poll, and J. Christophersen, "Prognostics methods for battery health monitoring using a Bayesian framework," *IEEE Trans. Instrum. Meas.*, vol. 58, no. 2, pp. 291–296, Feb. 2009.

[15] W. He, N. Williard, M. Osterman, and M. Pecht, "Prognostics of lithium-ion batteries based on Dempster–Shafer theory and the Bayesian Monte Carlo method," *J. Power Sources*, vol. 196, no. 23, pp. 10314–10321, Dec. 2011.

[16] Y. Xing, E. W. M. Ma, K.-L. Tsui, and M. Pecht, "An ensemble model for predicting the remaining useful performance of lithium-ion batteries," *Microelectron. Rel.*, vol. 53, pp. 811–820, Jun. 2013.

[17] A. Guha and A. Patra, "State of health estimation of lithium-ion batteries using capacity fade and internal resistance growth models," *IEEE Trans. Transport. Electrific.*, vol. 4, no. 1, pp. 135–146, Mar. 2018.

[18] F. Yang, D. Wang, Y. Xing, and K.-L. Tsui, "Prognostics of Li(NiMnCo)O_2-based lithium-ion batteries using a novel battery degradation model," *Microelectron. Rel.*, vol. 70, pp. 70–78, Mar. 2017.

[19] D. Wang, F. Yang, Y. Zhao, and K.-L. Tsui, "Battery remaining useful life prediction at different discharge rates," *Microelectron. Rel.*, vol. 78, pp. 212–219, Nov. 2017.

[20] J. Wu, C. Zhang, and Z. Chen, "An online method for lithium-ion battery remaining useful life estimation using importance sampling and neural networks," *Appl. Energy*, vol. 173, pp. 134–140, Jul. 2016.

[21] M. Jouin, R. Gouriveau, D. Hissel, M.-C. Péra, and N. Zerhouni, "Particle filter-based prognostics: Review, discussion and perspectives," *Mech. Syst. Signal Process.*, vols. 72–73, pp. 2–31, May 2016.

[22] P. L. T. Duong and N. Raghavan, "Heuristic Kalman optimized particle filter for remaining useful life prediction of lithium-ion battery," *Microelectron. Rel.*, vol. 81, pp. 232–243, Feb. 2018.

[23] W. Yan, B. Zhang, W. Dou, D. Liu, and Y. Peng, "Low-cost adaptive lebesgue sampling particle filtering approach for real-time li-ion battery diagnosis and prognosis," *IEEE Trans. Autom. Sci. Eng.*, vol. 14, no. 4, pp. 1601–1611, Oct. 2017.

[24] Q. Miao, L. Xie, H. Cui, W. Liang, and M. Pecht, "Remaining useful life prediction of lithium-ion battery with unscented particle filter technique," *Microelectron. Rel.*, vol. 53, pp. 805–810, Jun. 2013.

[25] X. Zhang, Q. Miao, and Z. Liu, "Remaining useful life prediction of lithium-ion battery using an improved UPF method based on MCMC," *Microelectron. Rel.*, vol. 75, pp. 288–295, Aug. 2017.

[26] H. Zhang, Q. Miao, X. Zhang, and Z. Liu, "An improved unscented particle filter approach for lithium-ion battery remaining useful life prediction," *Microelectron. Rel.*, vol. 81, pp. 288–298, Feb. 2018.

[27] Y. Ma, Y. Chen, X. Zhou, and H. Chen, "Remaining useful life prediction of lithium-ion battery based on gauss-hermite particle filter," *IEEE Trans. Control Syst. Technol.*, to be published.

[28] D. Z. Li, W. Wang, and F. Ismail, "A mutated particle filter technique for system state estimation and battery life prediction," *IEEE Trans. Instrum. Meas.*, vol. 63, no. 8, pp. 2034–2043, Aug. 2014.

[29] D. Wang, F. Yang, K.-L. Tsui, Q. Zhou, and S. J. Bae, "Remaining useful life prediction of lithium-ion batteries based on spherical cubature particle filter," *IEEE Trans. Instrum. Meas.*, vol. 65, no. 6, pp. 1282–1291, Jun. 2016.

[30] T. Li, S. Sun, T. P. Sattar, and J. M. Corchado, "Fight sample degeneracy and impoverishment in particle filters: A review of intelligent approaches," *Expert Syst. Appl.*, vol. 41, pp. 3944–3954, Jun. 2014.

[31] J. Yu, B. Mo, D. Tang, H. Liu, and J. Wan, "Remaining useful life prediction for lithium-ion batteries using a quantum particle swarm optimization-based particle filter," *Quality Eng.*, vol. 29, no. 3, pp. 536–546, May 2017.

[32] W. Zhou, L. Liu, and J. Hou, "Firefly algorithm-based particle filter for nonlinear systems," *Circuits, Syst., Signal Process.*, vol. 38, no. 4, pp. 1583–1595, Apr. 2019.
[33] X.-S. Yang, "A new metaheuristic bat-inspired algorithm," in *Nature Inspired Cooperative Strategies for Optimization*. Berlin, Germany: Springer, 2010, pp. 65–74.
[34] B. Bole, C. S. Kulkarni, and M. Daigle, "Adaptation of an electrochemistry-based Li-ion battery model to account for deterioration observed under randomized use," in *Proc. Annu. Conf. PHM Soc.*, Fort Worth, TX, USA, 2014, pp. 502–510.
[35] R. R. Richardson, M. A. Osborne, and D. A. Howey, "Gaussian process regression for forecasting battery state of health," *J. Power Sources*, vol. 357, pp. 209–219, Jul. 2017.
[36] J. Szoplik, "Forecasting of natural gas consumption with artificial neural networks," *Energy*, vol. 85, pp. 208–220, Jun. 2015.
[37] M. S. Arulampalam, S. Maskell, N. Gordon, and T. Clapp, "A tutorial on particle filters for online nonlinear/non-Gaussian Bayesian tracking," *IEEE Trans. Signal Process.*, vol. 50, no. 2, pp. 174–188, Feb. 2002.
[38] X.-S. Yang and A. H. Gandomi, "Bat algorithm: A novel approach for global engineering optimization," *Eng. Comput.*, vol. 29, no. 5, pp. 464–483, 2012.
[39] L. Zhang, Z. Mu, and C. Sun, "Remaining useful life prediction for lithium-ion batteries based on exponential model and particle filter," *IEEE Access*, vol. 6, pp. 17729–17740, 2018.

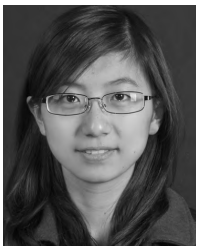

YI WU received the B.S. and M.S. degrees from the College of Automation Engineering, Nanjing University of Aeronautics and Astronautics, Nanjing, China, in 2010 and 2013, respectively, where she is currently pursuing the Ph.D. degree.

From 2015 to 2018, she was a Research Assistant with the Battery Group of the Center for Advanced Life Cycle Engineering, University of Maryland at College Park, College Park, MD, USA. Her research interests include failure analysis, health monitoring, and prognostics of lithium-ion batteries.

WEI LI is currently pursuing the Ph.D. degree with the Nanjing University of Aeronautics and Astronautics. From 2015 to 2017, he was a Visiting Ph.D. Student with the University of Kentucky. He is currently an Intern of the Baidu Research. His current research interests include artificial intelligence and deep learning.

YOUREN WANG was born in 1963. He is currently a Professor and a Ph.D. Supervisor with the College of Automation Engineering, Nanjing University of Aeronautics and Astronautics, Nanjing, China.

His research interests include mechanical and electrical system monitoring, fault diagnosis, remaining useful life prognosis, and intelligent health management.

KAI ZHANG received the B.S. degree in the measurement and control technology and instrument from the Heilongjiang University of Science and Technology, Harbin, China, in 2017.

He is currently pursuing the M.S. degree with the Nanjing University of Aeronautics and Astronautics, Nanjing, China. His research interests include fault diagnosis and health management of lithium-ion batteries.